Journal of Physics: Conference Series

PAPER • OPEN ACCESS

Influence of E85 on performance and efficiency of a motorcycle engine

To cite this article: C Di Gaetano *et al* 2023 *J. Phys.: Conf. Ser.* **2648** 012083

View the article online for updates and enhancements.

You may also like

- Choice at the pump: measuring preferences for lower-carbon combustion fuels
John P Helveston, Stephanie M Seki, Jihoon Min et al.
- Life cycle greenhouse gas impacts of ethanol, biomethane and limonene production from citrus waste
Mohammad Pourbafrani, Jon McKechnie, Heather L MacLean et al.
- Electrochemical Behavior of Oxide Ion in a LiCl – NaCl – $CaCl_2$ Eutectic Melt
Yuya Kado, Takuya Goto and Rika Hagiwara

This content was downloaded from IP address 155.185.56.86 on 29/02/2024 at 09:57

Influence of E85 on performance and efficiency of a motorcycle engine

C Di Gaetano[1], A Volza[1], S Caprioli[1], F Scrignoli[1], C A Rinaldini[1, a]
[1] Department of Engineering "Enzo Ferrari", University of Modena and Reggio Emilia, Italy
[a)] C.A.: carloalberto.rinaldini@unimore.it

Abstract

E85 (85 vol% ethanol and 15 vol% gasoline blend) is one of the most promising sustainable fuels for SI engines, thanks to the optimum trade-off between pollutant emissions and cost of implementation, starting from a pure gasoline baseline.

From the point of view of engine performance, the most relevant differences from such a baseline are related to the heat of vaporization and to the laminar flame speed. The higher heat of vaporization helps to reduce combustion temperature, thus the risk of knocking, but it also slows down the air-mixing process; the small amount of Oxygen in the fuel molecule leads to a slightly different combustion behavior.

The goal of this study is to compare commercial gasoline (E5, 5 vol% ethanol and 95 vol% gasoline blend) and E85, by means of CFD 1D (GT-Power) and 3D (AVL-FIRE) simulations, using experimentally calibrated models. The reference engine is a single-cylinder, four-stroke, PFI motorcycle unit, with a displacement of 463 cc and a maximum power > 30 kW at 9500 rpm.

After the calibration, carried out on the E5 version, the fuel type is changed to E85 in the 1D model, in order to provide accurate Initial Conditions (ICs) and Boundary Conditions (BNDs) to the CFD-3D analysis. Then, a series of combustion simulations are carried out at maximum power operative point (9500 rpm – WOT), varying spark advance and equivalence ratios.

Results reveal that an increase of fuel flow rate and a new calibration of spark timing are needed when the engine runs on E85 to reach performances comparable to the ones obtained with E5. Simulations also show that, moving from E5 to E85, combustion efficiency can be significantly increased, with a small reduction in engine performance.

An estimation of specific emissions, provided by ECFM-3Z combustion model, show that, using E85, CO and HC emissions can be significantly reduced with a small increase of NO emissions, compared to gasoline case.

Keywords: bioethanol, combustion, sustainability, motorcycle, Internal Combustion Engine

Content from this work may be used under the terms of the Creative Commons Attribution 3.0 licence. Any further distribution of this work must maintain attribution to the author(s) and the title of the work, journal citation and DOI.
Published under licence by IOP Publishing Ltd

Acronyms and symbols

E0	0 vol% ethanol – 100 vol% gasoline
E5	5 vol% ethanol – 95 vol% gasoline
E10	10 vol% ethanol – 90 vol% gasoline
E30	30 vol% ethanol – 70 vol% gasoline
E50	50 vol% ethanol – 50 vol% gasoline
E85	85 vol% ethanol – 15 vol% gasoline
SI	Spark Ignition
PFI	Port Fuel Injection
ICs	Initial Conditions
BNDs	Boundary Conditions
WOT	Wide Open Throttle
4S	4-Stroke
MTB	Maximum Brake Torque
BTE	Brake Thermal Efficiency
HC	Hydrocarbon
CO	Carbon Oxide
CO2	Carbon Dioxide
NOx	Nitrogen Oxides
LHV	Lower Heating Value
CFD	Computational Fluid Dynamics
IMEP	Indicated Mean Effective Pressure
BMEP	Brake Mean Effective Pressure
gIMEP	gross Indicated Mean Effective Pressure
FMEP	Friction Mean Effective Pressure
SA	Spark Advance
VE	Volumetric Efficiency
BSFC	Brake Specific Fuel Consumption
CAD	Crank Angle Degree
IVC	Intake Valve Close
IVO	Intake Valve Open
EVC	Exhaust Valve Close
EVO	Exhaust Valve Open
EGR	Exhaust Gas Recirculation
AHRR	Apparent Heat Release Rate
aFTDC	after Firing Top Dead Centre
MFB50	angle at 50% of Mass Fuel Burned
MFB10	angle at 10% of Mass Fuel Burned
MFB90	angle at 90% of Mass Fuel Burned
PPRR	Peak Pressure Rise Rate
Φ	Equivalence ratio

1. Introduction

Due to rising fuel prices, the need to reduce reliance on fossil fuels, growing energy demand, and stricter air pollution regulations in the road transport sector, researchers worldwide, both in industry and academia, are working towards developing clean and renewable fuels. Ethanol, with a global production of 120 billion liters in 2017 [1], and in particular bioethanol, constituting 65 % of worldwide biofuel output [2], plays a crucial role as a sustainable fuel.

To achieve the decarbonization targets in the road transport sector, a potential short-term solution is to mix conventional gasoline with renewable and environmentally friendly fuels, like (bio)ethanol. However, substituting gasoline with ethanol requires addressing some challenges. These include managing the different spray and evaporation behavior and ensuring combustion stability and performance.

Ethanol-gasoline blends can serve as alternative fuels for SI engines almost without the need for engine modifications, up to a blend of 35 vol% ethanol [3]. However, as the amount of ethanol increases, the pitting corrosion problem has to be evaluated, paying attention on the whole injection system. [4], [5]

Inbanaathan et al. [6] conducted an experimental study with various gasoline-ethanol blends (E10, E30, E50) analyzing combustion performance and emissions at various engine speeds. One of the main results regarding combustion behavior shows that E30 has maximum in-cylinder pressure very close to the gasoline ones for the considered operating point (1200, 1400, 1600, 1800 RPM). They also tested the addition of hydrogen to a blend containing 30 vol% of ethanol, in order to reduce pollutant emissions. The results demonstrate that the above-mentioned blend can be used as a substitute for gasoline in existing Spark Ignition (SI) engines.

Li et al. [7] investigated performance, combustion characteristics and emissions of a single-cylinder, 4S, SI engine fuelled with methanol, ethanol and butanol, blended with gasoline, at different equivalence ratios. They found that using E30 with spark time set to gasoline's MTB (Maximum Brake Torque), BTE (Brake Thermal Efficiency) decreases due to improper combustion phasing. This result combined with those obtained by Castagliola et al. [8] suggests that an adjustment of spark time and injection time could be necessary to achieve better efficiency and performance when ethanol blend increases.

As far as gaseous emissions produced by an engine fueled with gasoline-ethanol blends are concerned, studies available in literature generally indicate that increasing the ethanol fraction leads to a reductions of HC, CO, CO_2, and NO_x emissions [9], [10]. In detail, HC and CO emissions tend to decrease thanks to ethanol addition due to its oxygen content [11], while its higher hydrogen-to-carbon ratio with respect to gasoline permits to reduce CO_2 emissions. Moreover, the higher latent heat of evaporation of ethanol than that of gasoline guarantees lower NO_X emissions, as confirmed by references [12], [13] [7], [6], [14].

Goksel Kaya [12] tested a single-cylinder, 2-Stroke (2S), uniflow scavenged engine fuelled with E0, E10, E30, E50. Results show that HC, CO, CO_2 and NO_X decrease as the ethanol fraction in the fuel blend increases. Moreover, delivery ratio and scavenging efficiency increase because of the faster evaporation of the ethanol compared to gasoline.

Doğan et al. [13] carried out an experimental study on a single-cylinder, 4S, SI engine fuelled with E0, E10 and M10 (90 vol% gasoline and 10 vol% methanol). They found that HC, CO and CO_2 emissions are lower in comparison with pure gasoline.

However, it is important to note that the formation of acetaldehyde (C_2H_4O) and formaldehyde (CH_2O) may increase significantly [10]. These substances, although they are still under investigation about their effects on humans, could be associated to irritation, allergic contact dermatitis, cancer, pulmonary oedema [15] [16]. Therefore, modifications of exhaust gas treatment system could be needed. Furthermore, as noted by Daemme LC at al., motorcycles equipped with three-way catalytic converters, showed a notable increase in ammonia emissions during engine cold starts [17].

As demonstrated by Iodice et al. [18], during warm-up operating conditions, fuel consumption is influenced by two opposing factors when a gasoline-ethanol blend is employed. Due to the Lower Heating Value (LHV) of ethanol compared to gasoline, higher mass flow rates of gasoline-ethanol

mixture need to be injected as the ethanol fraction increases. However, despite the engine operates with rich air/fuel ratios during the cold transient phase, higher ethanol fractions can result in a leaning effect, which improves the combustion process. This phenomenon, known as "leaning effect," has also been studied by Hsieh et al., who demonstrated improved engine performance for blends up to 30 vol% ethanol [19]. Other important properties of ethanol are the higher octane number and the higher latent heat of evaporation with respect to gasoline. These properties can be leveraged to increase the compression ratio and the intake air density. Additionally, the higher laminar flame speed of ethanol leads to faster combustion, which further enhances thermodynamic efficiency.

In this study, experimentally validated 1D and 3D Computational Fluid Dynamics (CFD) gasoline models of a single cylinder, 4S motorcycle engine were employed to evaluate combustion characteristics when the engine is fueled with E85 (85 vol% ethanol and 15 vol% gasoline blend). Furthermore, various equivalence ratios and spark timings were compared at 9500 RPM + WOT operating point.

2. Methodology

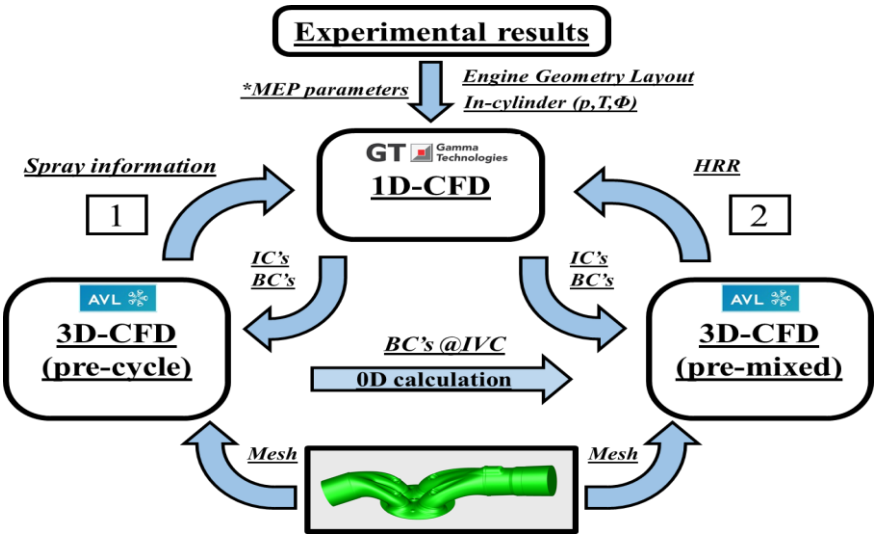

Figure 1: CFD simulation workflow.

Starting from geometric information of the engine, combustion-related data, as well as other mean and instantaneous experimental results obtained with a commercial gasoline (E5) at Wide Open Throttle (WOT), a preliminary 1D-CFD model has been built and validated in the GT-Power (by Gamma Technologies Inc) environment. The main features of the engine are listed in Table 1.

Table 1: Main features of the investigated engine

Engine Type	PFI-SI 4-Stroke
Fuel type	Gasoline (E5)
N. of cylinders	1
Bore x Stroke [mm]	96 x 64
Compression ratio	12.5
N. of valves per cylinder	2 + 2
Exhaust Valve Opening [CAD bBDC]	51
Intake Valve Opening [CAD bTDC]	15
Exhaust Valve Closing [CAD aTDC]	16
Intake Valve Closing [CAD aBDC]	56
Air Metering	Naturally aspirated

Once the 1D-CFD model has been experimentally validated, initial and boundary conditions have used in a 3D-CFD model of the engine built by means of AVL FIRE M software [20]. The fuel used during the experimental campaign is commercial gasoline (E5), which is modelled with $C_{7.93}H_{14.8}$ in the GT-Power model, while a 95 vol% isooctane and 5 vol% ethanol blend is employed in the 3D-CFD model as the gasoline surrogate.

A first iterative process between 1D and 3D-CFD simulations (represented by box "1" in Figure 1) ensures for more precise validation of the GT-Power model. In particular, a preliminary "pre-cycle" 3D-CFD simulation has been performed. Pre-cycle simulations, which approach is shown in Figure 2, consider the repetition of some engine cycle focusing the attention on the intake that is always active during this simulation [20]. These types of simulations are useful to study spray formation, wall film production and distribution inside intake system.

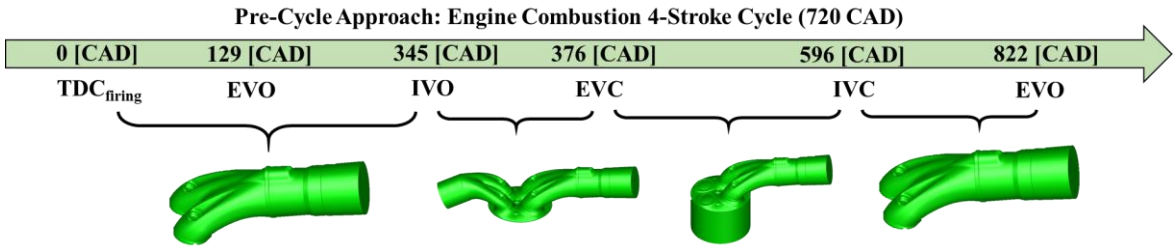

Figure 2: Pre-Cycle simulation approach

In this case a standard spray model with default parameters provided by software manual has been used in order to predict the amount of fuel which evaporate within the air during the cycle. The results obtained from the pre-cycle simulation feed the 1D-CFD model to improve its predictability and then accuracy of both initial and boundary conditions for the 3D-CFD combustion model.

A second iterative process (represented by box "2" in Figure 1), is carried out between 1D and 3D-CFD combustion simulations. In this case, 3D-CFD simulations (called pre-mixed) are mainly focused on the combustion process. In this approach, shown in Figure 3, a homogeneous air- fuel mixture characterized by a fixed equivalence ratio (Φ) is introduced in the intake domain (spray injection is not simulated). This assumption is based on the hypothesis that fuel has enough time to evaporate and thoroughly mix with air before the combustion process takes place.

Being the combustion the main interest in this kind of simulation, the cylinder volume is always active, while intake and exhaust domains are deactivated when the respectively valves are closed, ensuring a good trade-off between result accuracy and computational cost.

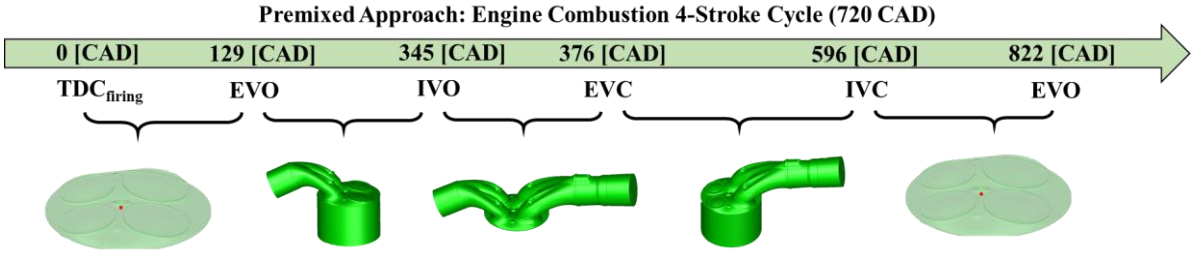

Figure 3: Premixed simulation approach

Four operative points (9500, 7000, 5000, 4000 rpm at full-throttle) are selected and then simulated in 3D-CFD environment, in order to calibrate some combustion model parameters (listed in section 4.2), which results are compared with 1D simulations, reducing the uncertainties related to experimental measurement.

The same workflow has been repeated for E85 for 9500 rpm – WOT operative point: passing from gasoline to E85, the equivalence ratio has been reduced from 1.186 to 0.930, based on an optimization process carried out on the GT-Power model, keeping the IMEP constant at 9500 rpm – WOT. Finally, a sensitivity analysis to the Spark Advance (SA) and Φ has been carried out at the same operating point.

For sake of brevity, the present paper is focused on CFD 1D and CFD 3D combustion simulations (pre-mixed) of E5 and E85; the CFD 3D pre-cycle simulations and the corresponding results are not reported, since they are discussed in a parallel paper.

3. 1D-CFD Engine model

Figure 4 depicts the GT-Power model of the investigated engine.

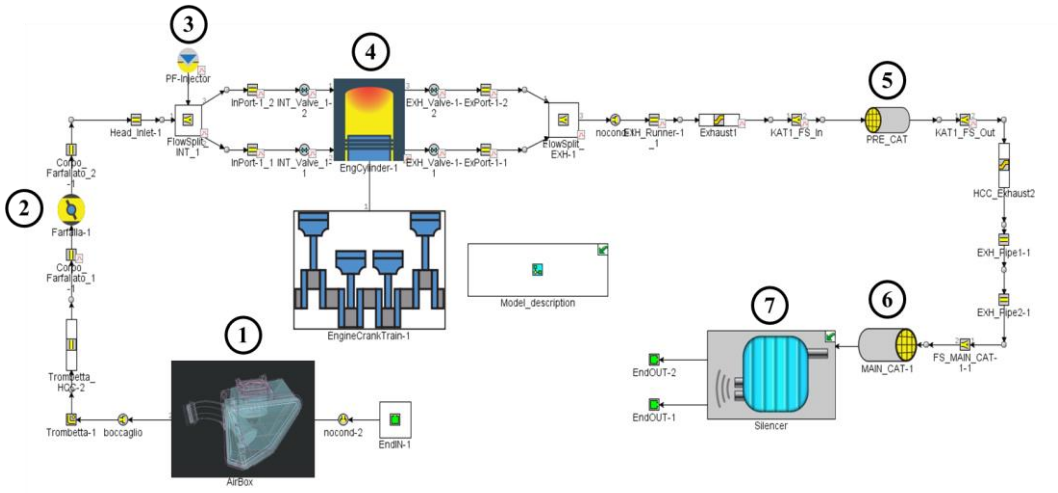

Figure 4: GT-Power model of the investigated engine.

1. Airbox
2. Throttle body
3. Port fuel injector
4. Cylinder (2 intake valves + 2 exhaust valves)
5. Pre-Catalyst brick
6. Main-Catalyst brick
7. Silencer

As described above, the test conditions at the dynamometer test-bench are replicated by means of the GT-Power model, in order to obtain a predictive 1D model of the engine. Burn-rate profiles with the experimental SA are implemented for all the considered engine operating points to ensure consistency in terms of combustion characteristics. Particular attention has been devoted to the calibration of the volumetric efficiency, which is fundamental to guarantee the correct amount of air and fuel trapped in the cylinder at each cycle. The main issues and variables calibrated in the GT-Power model validation process are:

- Accurate reproduction of strongly three-dimensional geometries (such as the airbox, intake and exhaust manifolds, and muffler)
- Distributed and concentrated losses along the intake, focusing on the taper

- Concentrated losses (filter, bell-mouth, discharge coefficients of throttle valve and intake/exhaust valves)
- dB-killer orifice diameter in order to match the experimental exhaust back-pressure
- Thermal exchange multiplier inside Woschni 0D Heat Transfer into cylinder object
- Intake and exhaust valve clearances.

Once a good agreement is achieved in terms of VE (Volumetric Efficiency), the gIMEP (gross Indicated Mean Effective Pressure) and the IMEP (Indicated Mean Effective Pressure) which are proportional to VE, have been calibrated by working on the heat-transfer multiplier, obtaining also a good match in terms of In-Cylinder Peak Pressure.

The friction losses, (Friction Mean Effective Pressure, FMEP), are calibrated using the empirical Chen-Flynn model, in order to obtain the experimental Brake Mean Effective Pressure (BMEP) and, consequently, all the "brake" quantities, such as Brake Specific Fuel Consumption (BSFC), Brake Torque and Brake Power, as shown in Figure 5.

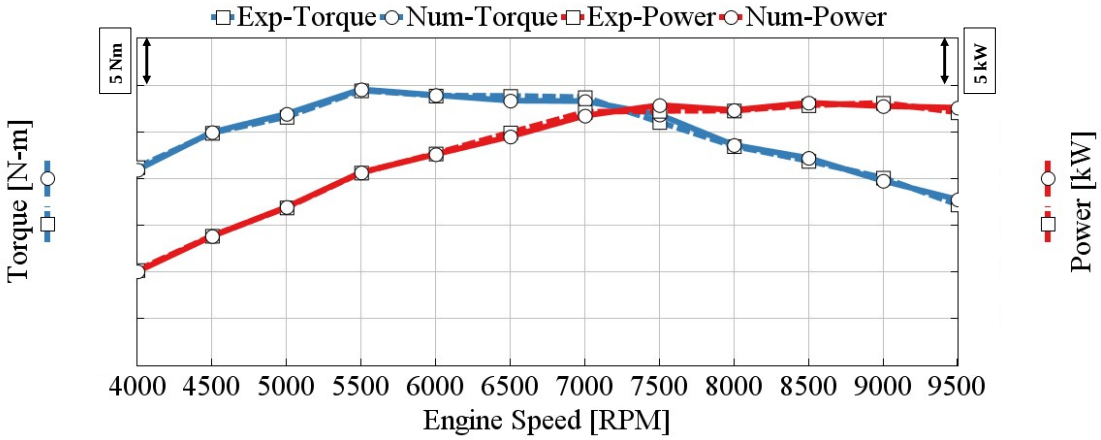

Figure 5: Comparison between experimental and numerical brake torque and power.

Other important results are reported in Figure 6. From top-left to bottom-right, VE, gIMEP, IMEP, peak in-cylinder pressure, BSFC and BMEP are shown. It is worth saying that all the considered parameters are normalized over the corresponding maximum value.

An error band has been introduced in the graphs to highlight the numerical deviation from the experimental results, over the whole speed range. The error band in dashed red lines is useful to understand how reliable could be a well calibrated numerical model compared to the experimental data, almost always affected by inevitable measurement uncertainties.

A satisfactory agreement is achieved by allowing for an acceptable margin of error between numerical simulation and experimental data for all the compared parameters. The maximum deviation (±5%) is obtained for VE and BSFC, followed by gIMEP and IMEP (±3%). The smaller error band, about ±2%, is calculated for In-Cylinder Peak Pressure and BMEP.

The varying error percentages indicate the tendency of certain variables of interest to be accurately captured by the one-dimensional code, while others, such as volumetric efficiency (VE), present greater challenges for extrapolation. In particular, it can be noted that there is a slight overestimation of the predicted trapped air mass at 4000 rpm – WOT. This discrepancy can be attributed to the use of linear trends in calibration factors over the engine speed range that makes it difficult for the 1D code to accurately capture intake pressure losses at very low engine speeds. However, the above-mentioned approach can be considered reliable, since it allows to correctly capture all the thermo-fluid dynamic phenomena of the engine.

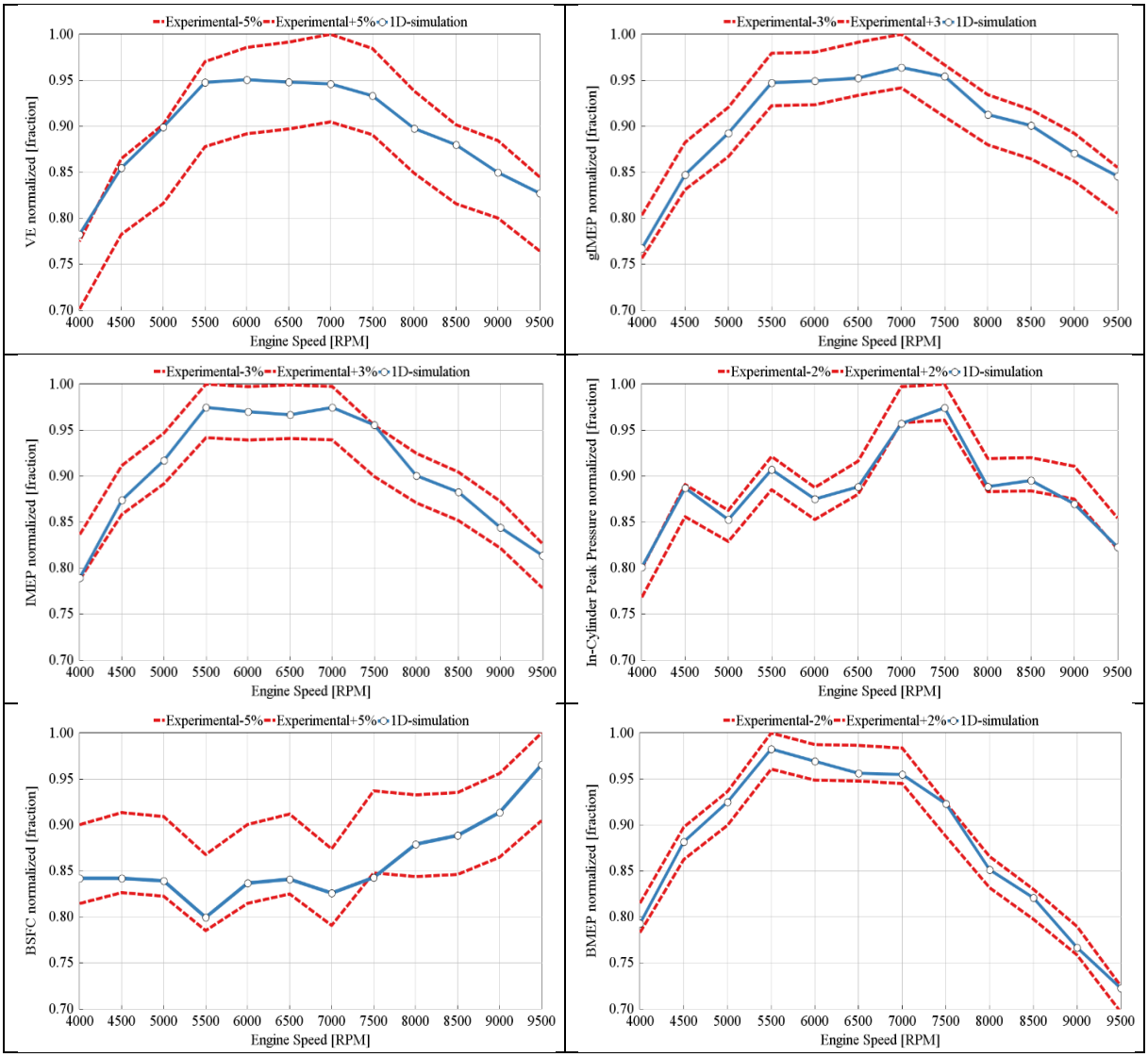

Figure 6: Main normalized calibration results of the reference engine 1D-numerical model. First row: Volumetric Efficiency (left) and gIMEP (right). Second row: IMEP (left) and In-Cylinder Peak pressure (right). Third row: BSFC (left) and BMEP (right).

Figure 7 reports the comparison between experimental and numerical in-cylinder pressure traces at four operating points:

- 4000 rpm (low end engine speed) – WOT
- 5000 rpm (medium-low engine speed) – WOT
- 7000 rpm (medium-high engine speed) – WOT
- 9500 rpm (maximum power engine speed) – WOT

As it can be seen, the GT-Power model is able to correctly predict in-cylinder pressure across the entire speed range of the engine.

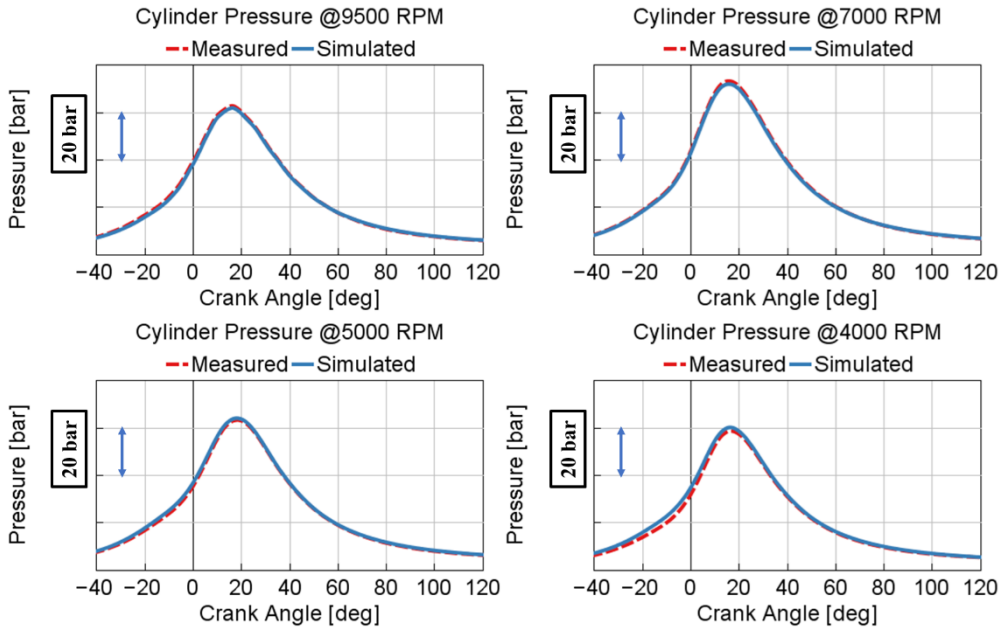

Figure 7: Cylinder pressure traces at various operating conditions for the reference engine: top-left 9500 rpm, top-right 7000 rpm, bottom-left 5000 rpm, bottom-right 4000 rpm

4. Gasoline (E5) 3D – CFD model

4.1. Computational Grid of the 3D CFD model of the engine

As previously said, the premixed combustion simulation approach has been employed in this study. In these simulations, only the combustion chamber is always active, since the focus of this type of simulation is the combustion process.

Based on the above-mentioned approach, four meshes have been created by means of AVL FIRE M, which features fully autonomous meshing. In detail, the following meshes have been built:

- Cylinder only moving mesh
- Exhaust port + cylinder moving mesh
- Intake and exhaust port + cylinder moving mesh
- Intake port + cylinder moving mesh.

Fixed refinements have been applied around the spark plug and the intake and exhaust valves stem and seats (see Figure 8), as well as for the injection cone, inlet and outlet boundaries. The number of cells varies between 500,000 and 2.5 million depending on the crank angle degree and on the activated volumes.

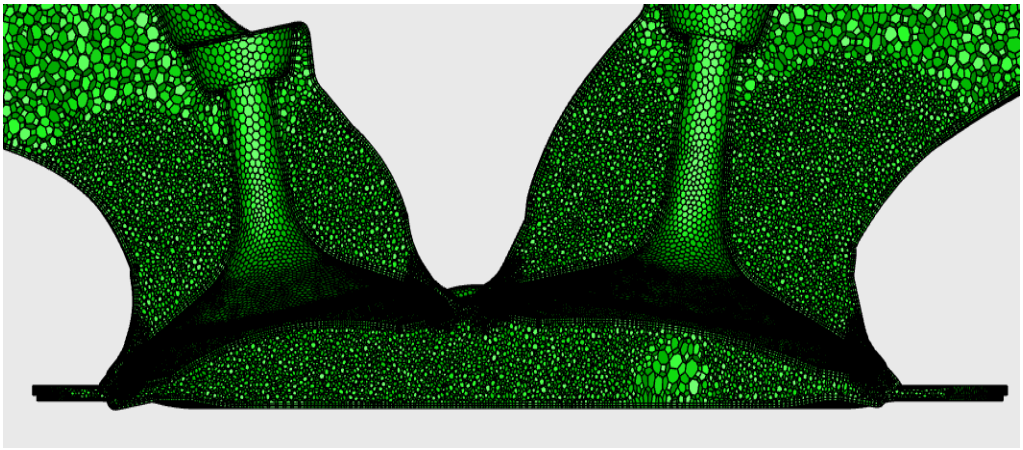

Figure 8: valve area mesh refinements section.

4.2. Gasoline (E5) Premix Combustion Simulation Setup

As already stated in the introduction section, this paper is focused on the results of the 3D combustion simulations (pre-mixed) of the engine running on different gasoline/ethanol blends E5 and E85.

After the first calibration loop between 1D and 3D-CFD pre-cycle simulations, reported in a parallel paper, boundary and initial conditions have been extracted by the GT-Power model and provided to the 3D-CFD premix model. Time varying total pressure and static temperature are imposed at the inlet boundary, while time varying static pressure is set at the outlet boundaries. Constant temperature boundaries have been applied to the walls of the fluid domain.

Table 2 lists the main models used in the 3D-CFD simulations described in this section.

Table 2: CFD-3D simulation main models

Simulation type	RANS
Turbulence model	k-zeta-f
Wall heat transfer model	Standard
Near wall treatment	Hybrid
Combustion model	ECFM-3Z
Ignition model	Spherical
Laminar Flame Speed	Metghalchi & Keck

Four operating points have been considered: 4000, 5000, 7000 and 9500 rpm – WOT. A first simulation is carried out from 270 to 839 CAD for each operating point to obtain pressure, temperature, velocity and mixture distribution before the start of combustion.

In order to reach the closest possible agreement between 1D and 3D results, reinitializations have been applied a few degrees after IVC. This is done setting coefficients that multiply pressure and/or temperature values of every cell in the region of interest in order to better comply with experimental results.

Charge composition can be reinitialized too specifying mass fraction values of each component or letting the software calculate them specifying equivalence ratio and EGR values. Once reinitialization is performed the mean value of the scalar involved is changed while the velocity and pressure fields are

conserved. It must be noted that reinitializations should be used to improve simulation accuracy only when multiplier factors are very close to 1, that is when calculated values are very closed to the target. Moreover, restart file has been saved a few crank angle degrees before SA with the aim to perform the combustion calibration.

4.3. Gasoline (E5) Premix Combustion Simulation Results

Figure 9 shows the comparison between 1D and 3D-CFD results in terms of in-cylinder pressure and Apparent Heat Release Rate (AHRR) for the operating point under investigation. Total trapped mass differences after reinitialization are lower than 1 %.

A good agreement has been obtained between 1D and 3D-CFD simulations, especially for the in-cylinder pressure traces, resulting in differences in terms of gIMEP* values within 5 % for each operating point simulated.

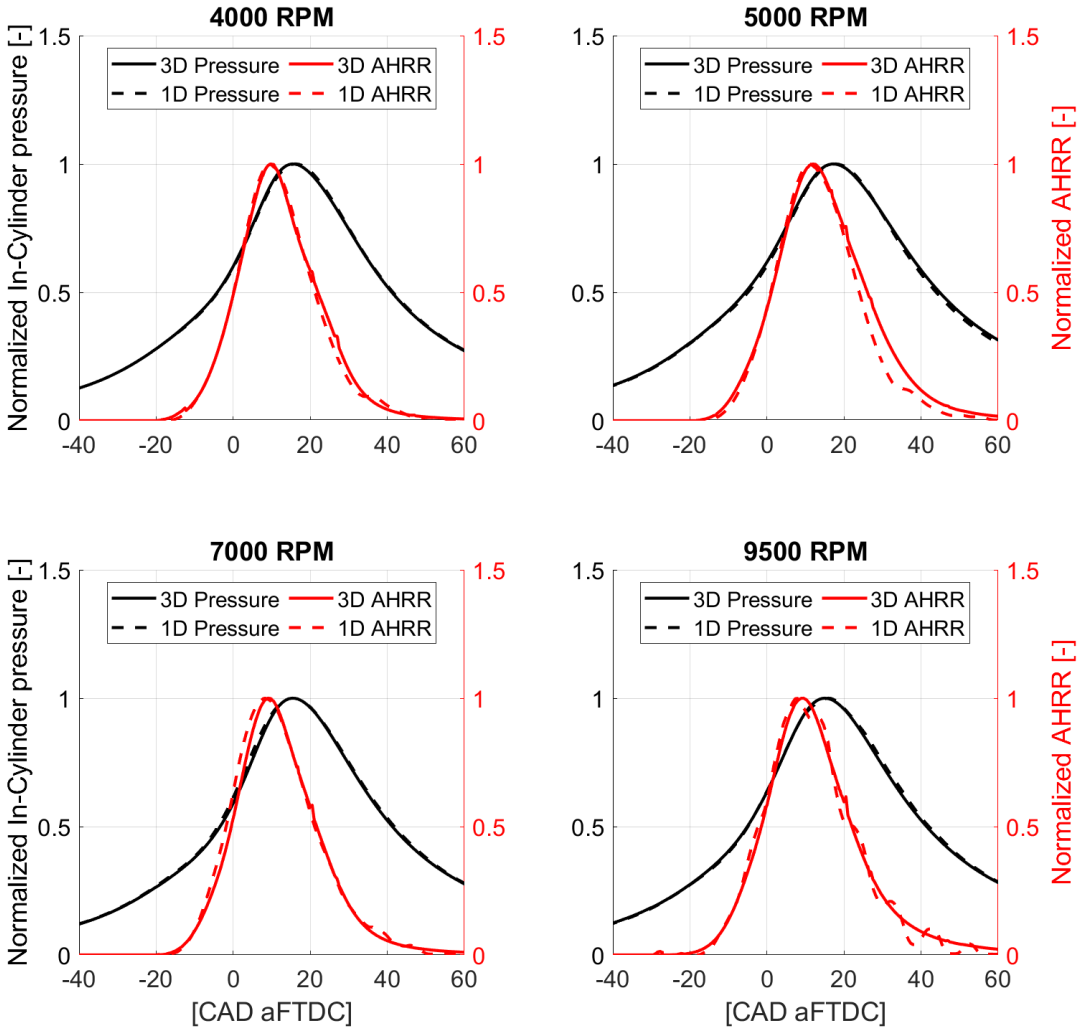

Figure 9: In-cylinder pressure and Apparent Heat Release Rate of 4000 (top-left), 5000 (top-right), 7000 (bottom-left) and 9500 (bottom-right) rpm cases.

A single set of values of the main combustion model (ECFM-3Z) parameters has been used for all the operating points investigated:

- Stretch factor: 0.69 [-]
- Initial Flame Surface Density: 1250 [1/m]
- Mixing model parameter: 1 [-]

Since premixed combustion simulations have been performed, the default value of the mixing model parameter, which influences air and unburnt fuel mixing velocity behind the flame front, i.e., diffusive combustion velocity, has been adopted.

SA values set in the 3D-CFD models are slightly different from the experimental values, as can be seen in Table 3. These differences can be attributed both to approximations of the numerical model and the uncertainties of the experimental SA.

The main performance parameters at 9500 rpm – WOT are summarized in Table 4.

Table 3: experimental and 3D model spark advance comparison

Operating point RPM	**Experimental spark advance** CAD aFTDC	**FIRE-M spark advance** CAD aFTDC
4000	-19.5	-19.5
5000	-15	-18.4
7000	-16	-20
9500	-25	-25

Table 4: 9500 case main performance parameters

Parameter	**Value**	**Unit**
gIMEP*	10.08	bar
Combustion efficiency	0.766	-
MFB50	10.25°	CAD aFTDC
Combustion duration (MFB10-90)	34°	CAD aFTDC
Equivalence ratio	1.186	-
Maximum in-cylinder pressure	62.44	bar
EGR	4	%

gIMEP* is evaluated from 651 to 800 CAD, while combustion efficiency is calculated with the following Equation 1:

$$\text{Combustion efficiency} = \frac{Q_c}{m_{f,tot} * LHV} \quad (1)$$

where Q_C is the heat released from combustion, $m_{f,tot}$ is the in-cylinder total fuel mass trapped and LHV is the lower heating value of the fuel.

Results indicate that the premixed combustion simulation provides accurate representation of the combustion process, since they are well calibrated with the 1D engine model which is a good representation of the experimental results.

Being 9500 rpm – WOT the operating point corresponding to maximum power, it has been chosen for combustion process investigations using E85 instead of gasoline (E5).

5. 3D – E85 Simulation setup

First of all, the gasoline surrogate has been substituted with E85 in the GT-Power model. The new boundary and initial conditions from the 1D-CFD model have been then provided to the AVL FIRE M model. The amount of fuel injected has been investigated through a GT-Power optimization, which returned an equivalence ratio equals to 0.93, instead of gasoline one which was 1.186. The objective of this optimization was to achieve Mean Effective Pressure (IMEP) as similar as possible to gasoline case, under the same 9500 rpm – WOT operative condition. Remember that due to different values of stoichiometric constants of E85 and E5, fuel mass of E85 increases for same equivalence ratios. The purpose of this article is to emphasize the modification of injection mass flow rate and ignition timing, in order to enable efficient fuel conversion without compromising performance and driving experience.

Moreover, it should consider that E85 is characterized by a significantly higher heat of evaporation compared to gasoline. Liquid fuels are exploited to reduce air temperature, thus, increase air density and volumetric efficiency. However, this is true when intake valves are opened. After IVC, evaporation of liquid fuel inside the cylinder only reduces air temperature without increasing the trapped mass. Furthermore, in a PFI engine, a part of the fuel evaporates after the contact with the intake walls, removing heat from walls rather than from air.

In order to take account of all these effects, two pre-cycle simulations, one for E5 and the second one for E85, at 9500 rpm – WOT have been performed to determine, for each blend, the mass fraction of fuel that evaporates, removing heat from air. For the sake of brevity, details of these simulations results are not discussed in this paper, while the calculated mass fractions (named Y_{E85} and Y_{E5}) are used in Equation 2, to approximate the air temperature decrease due to higher latent heat of evaporation of E85 compared to E5:

$$m_{air}\, c_{p,air}\, \Delta T = (m_{E85}\, h_{E85} Y_{E85} - m_{E5}\, h_{E5}\, Y_{E5}) \quad (2)$$

where m_{air}, m_{E85}, m_{E5} are the in-cylinder trapped mass of air, E85 and E5, respectively; $c_{p,air}$ is the constant pression specific heat; ΔT is the decrease of air temperature moving from E5 to E85; h_{E85} and h_{E5} are the latent heat of evaporation of E85 and E5, respectively, Y_{E85} and Y_{E5} are the E85 and E5 mass fractions of total injected fuel which participate to air temperature decrease.

Constant pressure specific heat of air and the latent heat of evaporation of E5 and E85 are assumed constant with temperature and evaluated at 300 K:

- $c_{c,air}$ = 1.041 kJ/(kg*K)
- h_{E85} = 837.68 kJ/kg
- h_{E5} = 341 kJ/kg

Rearranging equation 2, the following formula can be obtained:

$$\Delta T = \left[\frac{\Phi_{E85} * h_{E85}}{\left(\frac{A}{F}\right)_{s,E85}} Y_{E85} - \frac{\Phi_{E5} * h_{E5}}{\left(\frac{A}{F}\right)_{s,E5}} Y_{E5} \right] * \frac{1}{c_{p,air}} \qquad (3)$$

being $\left(\frac{A}{F}\right)_{s,E85}$ and $\left(\frac{A}{F}\right)_{s,E5}$ the stoichiometric air-to-fuel ratio assumed of E85 (9.799) and E5 (14.680), respectively.

5.1. 3D – E85 Premixed Combustion Simulation Results

In order to exploit the potential of E85 and its influence on combustion process, several premix simulations have been performed and results have been compared with ones obtained with E5. In particular, a sensitivity analysis is conducted by means of equivalence ratio and SA sweeps:

- Φ: 1.186, 1.1, 1, 0.95, 0.9, 0.8
- SA: – 50, – 45, – 40, –35, – 30, – 27, – 25, – 20, – 15 CAD

The results obtained from the sensitivity analysis have been compared with the reference case, namely, E5, Φ = 1.186 and SA = – 25 CAD aTDC.

It is important to note that E85 is investigated considering also lean mixture while the reference engine runs, in the investigated operating point, with a rich mixture. This is due to the fact that it is possible to supposed that the original engine runs on E5 with Φ>1 mainly to limit the knock risk; while, using E85, the risk of knocking is significantly reduced thanks to the higher Octane Number of the fuel and to the higher cooling effect of the fuel vaporization on the fresh charge, allowing to use slightly lean mixtures without the risk of knocking.

Figure 10 and Figure 11 show gIMEP* and combustion efficiency as a function of SA, for different values of Φ. As it can be seen, gIMEP* increases as SA is increased up to – 30/35 CAD aFTDC, depending on the Φ value. If SA is further increased, gIMEP* tends to decrease. The cases with Φ = 0.8 are characterized by a different trend. In detail, gIMEP* is always increasing as the SA is increased. It is also interesting to notice that gIMEP* increases as Φ is reduced from 1.186 to 1, regardless of SA. If Φ is further reduced (Φ = 0.8) gIMEP* drops, probably due to the significant reduction of the laminar flame speed of the air-fuel mixture. It can be also noticed that the gIMEP* of the reference case is higher than all E85 cases.

Combustion efficiency can be slightly increased if the SA is increased up to – 25 CAD aFTDC (– 30 CAD aFTDC if Φ = 0.8) for all the simulated values of Φ. Then, combustion efficiency remains almost constant if SA is further increased. As expected, combustion efficiency is strongly influenced by Φ: combustion efficiency decreases if Φ is increased, regardless of SA. In particular, when Φ>1 combustion efficiency cannot be greater than 1/Φ because of the lack of combustion air to complete the combustion process. It is interesting to noted that E85 cases with Φ=1.1 is characterized by a slightly lower combustion efficiency than the gasoline reference case Φ = 1.186, regardless of SA. It can be also noted that the E85 case with Φ = 0.8 is the only one able to reach an almost complete combustion if SA>30 CAD but, for lower SA values, combustion process gets worse and combustion efficiency drops.

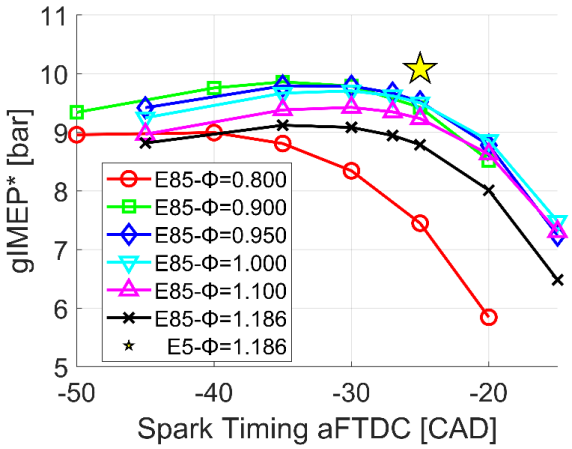

Figure 10: gIMEP* vs Spark Advance at each equivalence ratio.

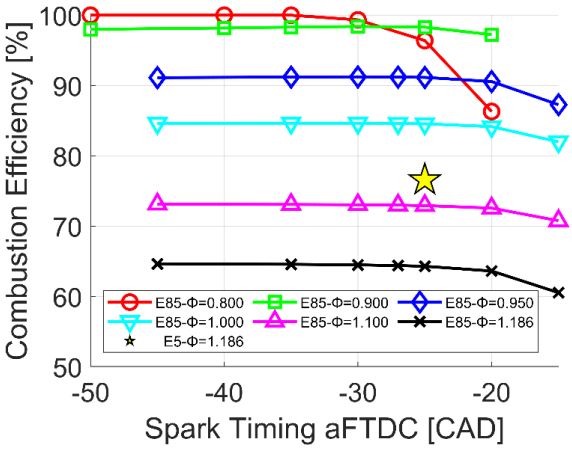

Figure 11: combustion efficiency vs Spark Advance at each equivalence ratio.

Based on the above-mentioned results, when the engine is fuelled with E85, performance can be maximized setting Φ in the range between 0.9 and 0.95, and SA between – 35° and – 30°.

Looking at Figure12, it is possible to note that E85 cases with SA = – 25 CAD aFTDC and Φ in the range between 1.1 and 0.95 show similar peak in-cylinder pressure of the gasoline reference case (62.44 bar).

When Φ is equal to 0.9 and 1.186, and SA = – 25 CAD aFTDC, peak in-cylinder pressure is slightly lower than in the gasoline reference case, while when Φ = 0.8, and SA = – 25 CAD aFTDC, peak in-cylinder pressure strongly decreases with respect to the reference E5 case. Furthermore, regardless of Φ, peak in-cylinder pressure increases as SA is increased from – 15 to – 50 CAD aFTDC.

A similar trend can be observed for Peak Pressure Rise Rate (PPRR), as it can be seen in Figure 13. It is interesting to note that all E85 cases, except for those ones with SA higher than – 40 CAD aTDC and Φ in the range between 0.9 and 1.186, PPRR is lower than 5 bar/CAD, which correspond to acceptable levels of vibration and noise for series engines.

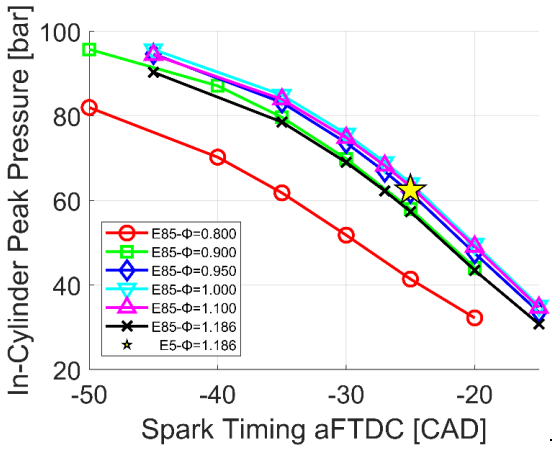

Figure 12: max mean cylinder pressure vs Spark Advance at each equivalence ratio.

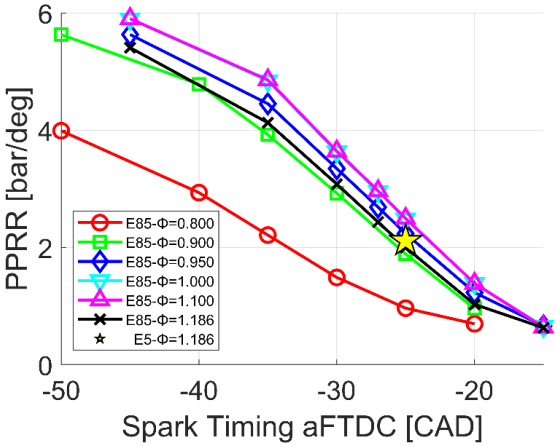

Figure 13: Peak Pressure Rise Rate comparison.

Peak in-cylinder pressure and PPRR behavior can be explained by looking at MFB50 and turbulent combustion duration (MFB10-90), which are depicted in Figures 14 and 15.

E85 cases with Φ in the range from 0.9 to 1.186, and SA = – 25 CAD aTDC, show similar MFB50 and slightly lower MFB10-90 with respect to the reference gasoline case.

Only the case with Φ = 0.8 is characterized by strongly different (higher) MFB50 and MFB10-90 compared to the reference case. Moreover, regardless of Φ, combustion duration and the center of mass of combustion decrease as SA is increased.

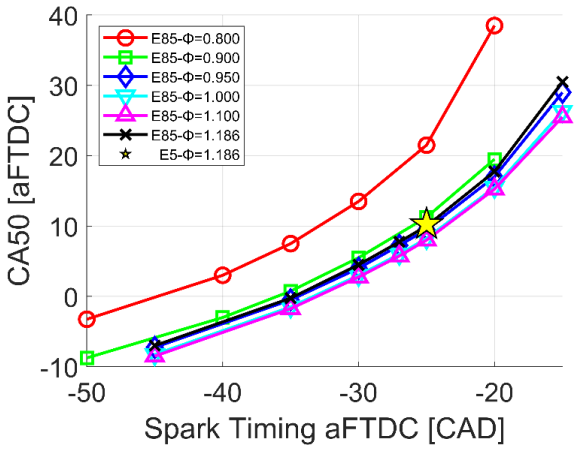

Figure 14: Crank angle at 50 % of fuel burned vs spark advance at each equivalence ratio.

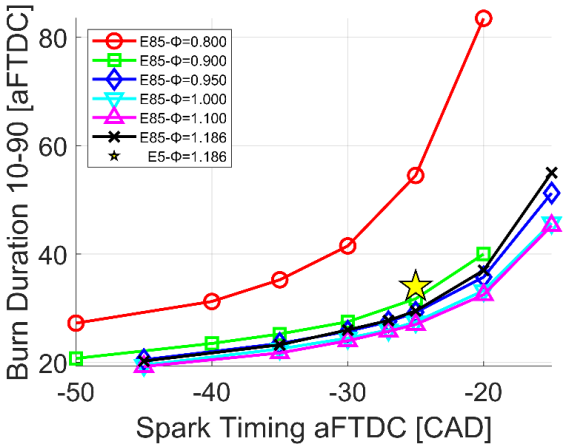

Figure 15: Turbulent combustion duration (MFB10-90) vs spark advance at each equivalence ratio.

Table 5 compares the results of the best E85 cases (named from I to IV) to the reference case (E5). The best E85 cases are characterized by slightly lower gIMEP* than E5 case (reductions from 2.2 to 2.9 %) but generally higher combustion efficiency (increases from 16% to 22.2%). However, regarding the combustion efficiency, it is important to remember that, in the case of a rich mixture (such as for E5), there is an excess of fuel compared to the amount of oxygen available for complete combustion and then combustion efficiency is usually expected lower compared to a stoichiometric or lean mixture (such as for E85). To consider that, for rich mixture, some of the fuel does not have sufficient oxygen to fully react, Table 5 reports, for the case of rich mixture of E5, also the value of the combustion efficiency multiplied by Φ.

The combustion efficiency multiplied by Φ for the case of rich mixtures represents the amount of fuel burnt divided not by the total amount of fuel trapped in the cylinder (as in the combustion efficiency) but only to the amount of fuel that can be burned with the trapped combustion air. Table 5 shows that considering that new parameter for the E5 mixture, moving from E5 to E85, combustion efficiency still increase for case I and II and remains almost constant for case III and IV. Finally, Tables 5 shows also that the use of E85 generally increase in-cylinder pressure from about 7 bar (case I) to about 21 bar (case IV).

Table 5: gIMEP*, combustion efficiency, max pressure comparison

Case	PHI	Spark Advance	gIMEP*	Combustion efficiency	Combustion efficiency*PHI	Max Pressure
	[-]	[CAD aFTDC]	[bar]	[-]	[-]	[bar]
E5	1.186	-25	10.08	0.766	0.908	62.44
I	0.9	-30	9.787 (-2.9%)	0.984 (+22.2%)	0.984 (+7.7%)	69.86 (+10.6 %)
II	0.9	-35	9.859 (-2.2%)	0.983 (+22.1%)	0.983 (+7.6%)	78.69 (+20.7 %)
III	0.95	-30	9.788 (-2.9%)	0.912 (+16.0%)	0.912 (+0.4%)	73.64 (+15.2 %)
IV	0.95	-35	9.791 (-2.9%)	0.912 (+16.0%)	0.912 (+0.4%)	83.17 (+24.9 %)

5.2. Specific emissions

This section provides a comparative estimation of the specific emissions, given by ECFM-3Z combustion model, of the four best cases shown above respect to gasoline case.

As can be seen in Figure 16, fueling with E85 can significantly decrease HC and CO emissions, while NO emissions increase slightly.

These results can be explained by the air/fuel ratio which value strongly influences combustion process and emissions:

- Values of Φ lower that 1 ensure an excess of air in respect to what is strictly necessary to completely burn the trapped fuel, which promote the oxidation process.
- Values of Φ greater than 1 lead necessary to the formation of unburned gases.

NO emissions increment is due to higher temperature reached during combustion. This is coherent with higher in cylinder pressure found in simulation results.

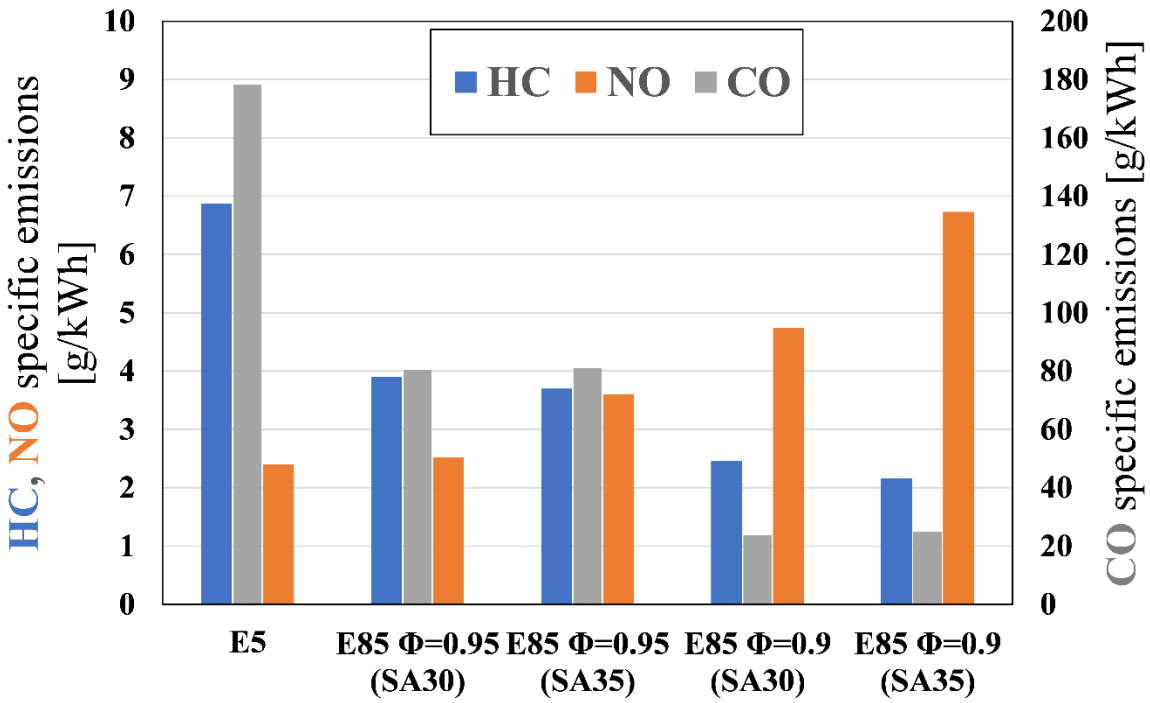

Figure 16: specific emissions of the four best cases compared to gasoline case.

Conclusions

The substitution of gasoline with E85 in a commercial, single cylinder, 4-Stroke internal combustion engine has been numerically investigated. Starting from an experimentally validated 1D-CFD model, a set of 3D-CFD premixed combustion simulations at four engine speed at WOT have been carried out when fueled with E5. After calibrating E5 3D combustion model, a new 1D-3D correlation with E85 has been done for 9500 rpm at WOT operating point. An air temperature decrease, due to higher latent heat vaporization of E85 compared to E5, has been evaluated using an equation based on parameters calculated in previous simulations. A number of 40 cases with E85 fuel have been simulated in 3D environment sweeping equivalence ratio and spark advance.

Results can be summarized as follow:

- An adjustment of SA and equivalence ratio is needed, compared to gasoline case base, to improve performance when fueling the engine with E85
- For same SA, reducing equivalence ratio increases combustion efficiency for Φ values up to 0.9
- Combustion efficiency can be increased up to 22% compared to gasoline case
- Higher laminar flame speed of E85, compared to gasoline, causes higher in-cylinder peak pressure and lower turbulent combustion duration
- PPRR values increase but remain under acceptance values with E85
- IMEP (thus performance) is slightly reduced when running with E85
- CO and HC emissions could be reduced with a small NO production increase.

It can be concluded that E85 can efficiently replace E5, strongly reducing the CO_2 footprint of the engine, when ethanol is derived from a biomass. The conversion of the engine requires an adjustment of fuel flow rate and spark advance while E85 characteristic can be successfully exploited to strongly limit the performance loss due to its lower LHV.

References

[1] P. Bajpai, *Developments in Bioethanol*. Springer Nature, 2020.
[2] A. Dufey, *Biofuels Production, Trade and Sustainable Development: Emerging Issues*. IIED, 2006.
[3] A. F. Kheiralla, M. El-Awad, M. Y. Hassan, M. A. Hussen, and H. I. Osman, 'Effect of ethanol-gasoline blends on fuel properties characteristics of spark ignition engines', *University Of Khartoum Engineering Journal*, vol. 1, no. 2, 2011.
[4] 'Surface Corrosion in Ethanol Fuel Pumps on JSTOR'. https://www.jstor.org/stable/44731593 (accessed Jul. 02, 2023).
[5] Y. Wan *et al.*, 'Influence of Ethanol on Pitting Corrosion Behavior of Stainless Steel for Bioethanol Fermentation Tanks', *Frontiers in Chemistry*, vol. 8, 2020, Accessed: Jul. 02, 2023. [Online]. Available: https://www.frontiersin.org/articles/10.3389/fchem.2020.00529
[6] P. V. Inbanaathan *et al.*, 'Comprehensive study on using hydrogen-gasoline-ethanol blends as flexible fuels in an existing variable speed SI engine', *International Journal of Hydrogen Energy*, Apr. 2023, doi: 10.1016/j.ijhydene.2023.03.107.
[7] Y. Li, J. Gong, Y. Deng, W. Yuan, J. Fu, and B. Zhang, 'Experimental comparative study on combustion, performance and emissions characteristics of methanol, ethanol and butanol in a spark ignition engine', *Applied Thermal Engineering*, vol. 115, pp. 53–63, Mar. 2017, doi: 10.1016/j.applthermaleng.2016.12.037.
[8] M. A. Costagliola *et al.*, 'Performances and emissions of a 4-stroke motorcycle fuelled with ethanol/gasoline blends', *Fuel*, vol. 183, pp. 470–477, Nov. 2016, doi: 10.1016/j.fuel.2016.06.105.
[9] X. Wang *et al.*, 'Evaluation of hydrous ethanol as a fuel for internal combustion engines: A review', *Renewable Energy*, vol. 194, pp. 504–525, Jul. 2022, doi: 10.1016/j.renene.2022.05.132.
[10] V. N. Duy, K. N. Duc, D. N. Cong, H. N. Xa, and T. Le Anh, 'Experimental study on improving performance and emission characteristics of used motorcycle fueled with ethanol by exhaust gas heating transfer system', *Energy for Sustainable Development*, vol. 51, pp. 56–62, Aug. 2019, doi: 10.1016/j.esd.2019.05.006.
[11] M. Koç, Y. Sekmen, T. Topgül, and H. S. Yücesu, 'The effects of ethanol–unleaded gasoline blends on engine performance and exhaust emissions in a spark-ignition engine', *Renewable Energy*, vol. 34, no. 10, pp. 2101–2106, Oct. 2009, doi: 10.1016/j.renene.2009.01.018.
[12] G. Kaya, 'Experimental comparative study on combustion, performance and emissions characteristics of ethanol-gasoline blends in a two stroke uniflow gasoline engine', *Fuel*, vol. 317, p. 120917, Jun. 2022, doi: 10.1016/j.fuel.2021.120917.
[13] B. Doğan, M. K. YeşiLyurt, D. Erol, and A. Çakmak, 'A Study Toward Analyzing the Energy, Exergy and Sustainability Index Based on Performance and Exhaust Emission Characteristics of a Spark-Ignition Engine Fuelled with the Binary Blends of Gasoline and Methanol or Ethanol', *Uluslararası Muhendislik Arastirma ve Gelistirme Dergisi*, pp. 529–548, Jun. 2020, doi: 10.29137/umagd.728802.
[14] M. Koç, Y. Sekmen, T. Topgül, and H. S. Yücesu, 'The effects of ethanol–unleaded gasoline blends on engine performance and exhaust emissions in a spark-ignition engine', *Renewable Energy*, vol. 34, no. 10, pp. 2101–2106, Oct. 2009, doi: 10.1016/j.renene.2009.01.018.
[15] World Health Organitation, 'Environmental Health Criteria 167'. WHO. [Online]. Available: https://apps.who.int/iris/bitstream/handle/10665/37962/9241571675-eng.pdf?sequence=1
[16] Mahdieh Delikhoon,a Mehdi Fazlzadeh,b,e Armin Sorooshian,c,d Abbas Norouzian Baghani,e,f,* Mohammad Golaki,g Qadir Ashournejad,h and Abdullah Barkhordarii, 'Characteristics and health effects of formaldehyde and acetaldehyde in an urban area in Iran'. [Online]. Available: https://www.ncbi.nlm.nih.gov/pmc/articles/PMC6221454/

[17] L. C. Daemme, R. Penteado, F. Zotin, and M. Errera, 'Regulated and Unregulated Emissions from a Flex Fuel Motorcycle Fuelled with Various Gasoline/Ethanol Blends', SAE International, Warrendale, PA, SAE Technical Paper 2014-32–0032, Nov. 2014. doi: 10.4271/2014-32-0032.
[18] P. Iodice, G. Langella, and A. Amoresano, 'Ethanol in gasoline fuel blends: Effect on fuel consumption and engine out emissions of SI engines in cold operating conditions', *Applied Thermal Engineering*, vol. 130, pp. 1081–1089, Feb. 2018, doi: 10.1016/j.applthermaleng.2017.11.090.
[19] W.-D. Hsieh, R.-H. Chen, T.-L. Wu, and T.-H. Lin, 'Engine performance and pollutant emission of an SI engine using ethanol–gasoline blended fuels', *Atmospheric Environment*, vol. 36, no. 3, pp. 403–410, Jan. 2002, doi: 10.1016/S1352-2310(01)00508-8.
[20] AVL, 'FIRE-M'.

Acknowledgments

Gamma Technologies is acknowledged for the GT-Power license granted to the University of Modena and Reggio Emilia used in this study.

AVL is acknowledged for the FIRE M license granted to the University of Modena and Reggio Emilia used in this study.